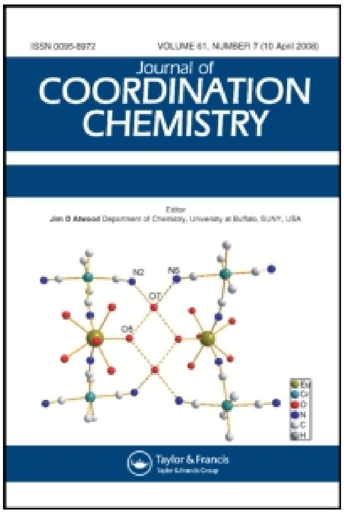

Journal of Coordination Chemistry
Publication details, including instructions for authors and subscription information:
http://www.informaworld.com/smpp/title~content=t713455674

Synthesis, characterization, ion-exchange and antimicrobial study of poly[(2-hydroxy-4-butoxy benzophenone)ethylene] resin and its polychelates with lanthanides

Malav Kapadia[a]; Mihir Patel[a]; Gautam Patel[a]; Jayantilal Joshi[a]
[a] Department of Chemistry, Sardar Patel University, Vidyanagar-388 120, Gujarat, India

To cite this Article Kapadia, Malav , Patel, Mihir , Patel, Gautam and Joshi, Jayantilal(2008) 'Synthesis, characterization, ion-exchange and antimicrobial study of poly[(2-hydroxy-4-butoxy benzophenone)ethylene] resin and its polychelates with lanthanides', Journal of Coordination Chemistry, 61: 5, 677 — 691, First published on: 04 September 2007 (iFirst)
To link to this Article: DOI: 10.1080/00958970701391290
URL: http://dx.doi.org/10.1080/00958970701391290

Journal of Coordination Chemistry
Vol. 61, No. 5, 10 March 2008, 677–691

Taylor & Francis
Taylor & Francis Group

Synthesis, characterization, ion-exchange and antimicrobial study of poly[(2-hydroxy-4-butoxy benzophenone)ethylene] resin and its polychelates with lanthanides

MALAV KAPADIA, MIHIR PATEL,
GAUTAM PATEL and JAYANTILAL JOSHI*

Department of Chemistry, Sardar Patel University, Vallabh,
Vidyanagar – 388 120, Gujarat, India

(*Received 5 February 2007; in final form 19 February 2007*)

The polymeric ligand (resin) was prepared from 2-hydroxy-4-butoxy benzophenone with ethane diol with polyphosphoric acid as catalyst on constant heating at 160°C for 13 h. The poly[(2-hydroxy-4-butoxy benzophenone)ethylene] (HBBP-ED) forms 1 : 2 metal : ligand polychelates with La(III), Pr(III), Nd(III), Sm(III), Gd(III), Tb(III) and Dy(III). The polymeric ligand and its polychelates were characterized by elemental analyses, electronic spectra, magnetic susceptibilities, IR-spectroscopy, NMR and thermogravimetric analyses. The molecular weight was determined using number average molecular weight ($\overline{M}n$) by a vapor pressure osmometry (VPO) method. All the polychelates are paramagnetic except La(III). Ion-exchange studies at different electrolyte concentrations, pH and rate have been carried out for the lanthanide ions. The resin can be used as an ion-exchanger and antimicrobial agent.

Keywords: Poly[(2-hydroxy-4-butoxy benzophenone)ethylene]; Lanthanide(III) polychelates; Thermal study; Ion-exchange; Antimicrobial study

1. Introduction

Organic ligands containing acidic phenol or carboxyl groups complex radionuclides under a variety of conditions [1, 2]. Such ligands form remarkably stable complexes; association of organic and inorganic units afford a new type of material with strong bonds, which resists cleavage reactions, provides multiple sites for attachment of a wide variety of ligands and high thermal stability.

Polymer-metal complexes attract interest in many scientific and technological fields. Coordination polymers have been prepared from aromatic and aliphatic polymers containing pendant functional groups which chelate in binding polyvalent metal ions [3]. Chelate-forming polymers [4–6] have found widespread applications in the separation and monitoring of heavy metals, including lanthanides [7], from aqueous solutions; they show significant applications in pollution control [8], bioinorganic

---

*Corresponding author. Tel.: +91 2692 226857 *221. Email: jdjoshi314@gmail.com

Journal of Coordination Chemistry
ISSN 0095-8972 print/ISSN 1029-0389 online © 2008 Taylor & Francis
DOI: 10.1080/00958970701391290

industry, water purification and selective removal of waste materials in nuclear plants [9–11], preconcentration [12] and hydrometallurgy [13]. The chelates of phenols possess interesting microbial activities like growth inhibition and acceleration. Polymeric coordinating reagents are novel substances possessing a combination of physical properties of a polymer and chemical properties of the attached reagent.

Considerable effort has been directed toward the improvement and optimization of chelating ion-exchange resins. Ion exchange materials are insoluble substances containing loosely held ions which are able to be exchanged with other ions in solutions that come in contact with them. These exchanges take place without physical alteration to the ion exchange material. Ion exchangers are insoluble acids or bases which have insoluble salts, and this enables them to exchange either positively charged ions (cation exchangers) or negatively charged ones (anion exchangers). Solid ion exchange particles are either naturally occurring or synthetically prepared. Synthetic resins are predominantly used as cation exchangers. Cation-exchange resins can also be used as fillers. It is also found that ion exchangers have a positive effect on water absorption and more durable and weather-resistant products are needed [14].

In the present work, an attempt has been made to study antimicrobial activity and ion-exchange capacity of the resin to exchange lanthanides; La(III), Pr(III), Nd(III), Sm(III), Gd(III), Tb(III) and Dy(III) polychelates with poly[(2-hydroxy-4-butoxy benzophenone)ethylene] have been examined. The polychelates are thermally less stable than the polymeric ligand and show excellent bactericidal activity compared to the parent polymeric ligand. Thus, looking to their effective behavior, lanthanide polychelates may be used as antibacterial agents.

2. Experimental

2.1. *Synthesis of resin*

All chemicals used were AR grade. To a well-stirred and ice-cooled mixture of 2-hydroxy-4-butoxy benzophenone (HBBP, Aldrich) (9.12 gm, 0.04 mol) and ethane diol (Aldrich, ED) (2.48 mL, 0.04 mol), polyphosphoric acid (Lancaster) (PPA) (20 gm) was added slowly with stirring as a catalyst. The reaction mixture was left at room temperature for 30 min and heated on an oil bath at 160°C for 13 h. The reaction mixture was then cooled, poured on crushed ice and left overnight. A blackish-brown solid separated out, was collected by filtration and washed with cold water and methanol to remove unreacted acid and monomer. The polymer was purified by reprecipitation from dimethyl formamide with water (three times) and dried at 60°C. The polymer was reddish brown in color, m.p. >270°C, yield 5.54 gm (60.7%). The reaction is shown in scheme 1.

2.2. *Synthesis of polychelates*

All polychelates were synthesized by a general method using lanthanum, praseodymium, neodymium, samarium, gadolinium, terbium and dysprosium acetates (Merck), AR grade.

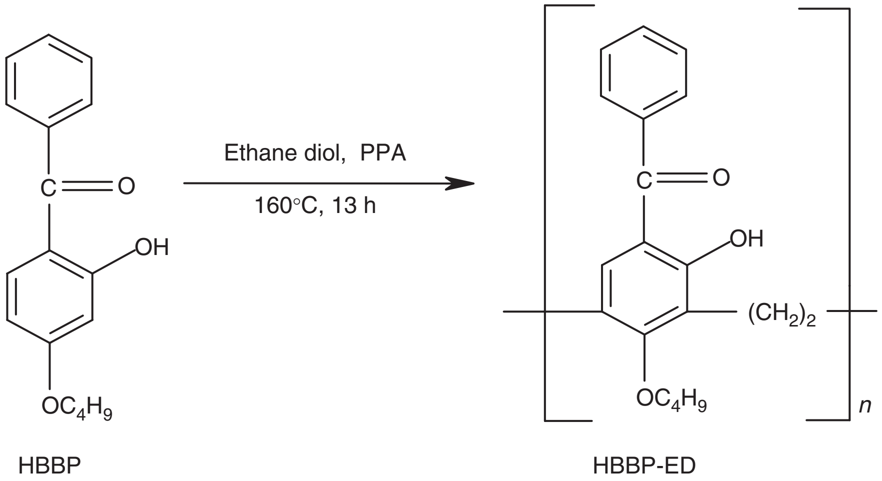

Scheme 1. Reaction for the preparation of resin.

The polymeric ligand (0.01 mol) was dissolved in DMSO (50 mL). The metal acetate (0.005 mol) was also dissolved in DMSO (25 mL). The hot and clear solution of the metal acetate was added with constant stirring to the hot and clear solution of ligand. A reddish-brown colored product separated immediately. The suspension was digested on a water bath at 90°C for 2 h and then filtered. The solid was washed with hot DMSO to remove unreacted metal acetate. Finally, the product was washed with acetone and dried at 60°C for 24 h. The yield of each polychelate was between 60–80%.

2.3. *Analytical procedures*

Carbon and hydrogen were analyzed with a Coleman C, H, N analyzer (table 1). The metal content was determined by titration with standard disodium salt of EDTA after decomposing the polychelates with a mixture of concentrated hydrochloric acid, sulfuric acid and perchloric acid in a 5 : 2 : 3 mL ratio. Magnetic susceptibilities were measured by the Gouy method at room temperature. The IR spectra of the samples in KBr pellets were recorded on a model 938 Perkin-Elmer spectrophotometer. Thermal measurements were performed using a Du Pont thermal analyzer at $10^\circ\mathrm{C\,min^{-1}}$ heating rate. ^{1}H NMR spectra were determined in DMSO-d_6 with a FT NMR spectrophotometer using TMS as an internal reference. The number average molecular weight ($\overline{M}n$) of polymeric ligand (resin) was measured with a Knaur Germany (VPO) using DMF as solvent at 90°C and polystyrene (PS) as a calibrant.

3. Results and discussion

3.1. *Infrared spectra*

The broad band appearing in the range $3300–3500\,\mathrm{cm^{-1}}$ is due to –O–H stretching from the phenolic hydroxyl group and water absorbed by resins. The major contribution to

Table 1. Analytical data and physical properties of the polymeric ligand and its polychelates.

Compound	Color	Formula weight of repeating unit	Yield (gm) (%)	(%) Found (Calculated) M	(%) Found (Calculated) C	(%) Found (Calculated) H	μ_{eff} (BM>)	D.P.^{b} (°C)
$(HBBP\text{-}ED)_n$	Reddish	296	5.00	–	77.00	6.80	–	>280
$[C_{19}H_{20}O_3]_n$	Brown		(50)		(77.02)	(6.81)		
$[La(HBBP\text{-}ED)_2(H_2O)_2]_n$	Reddish	765	3.18	18.20	59.61	5.52	Diamagnetic	>300
$[C_{38}H_{42}O_8La]_n$	Brown		(70)	(18.17)	(59.59)	(5.50)		
$[Pr(HBBP\text{-}ED)_2(H_2O_2)]_n$	Reddish	766	3.27	18.35	59.45	5.51	3.72	>350
$[C_{38}H_{42}O_8Pr]_n$	Brown		(68)	(18.33)	(59.48)	(5.49)		
$[Nd(HBBP\text{-}ED)_2(H_2O)_2]_n$	Reddish	770	3.23	18.70	59.19	5.49	3.61	>350
$[C_{38}H_{42}O_8Nd]_n$	Brown		(71)	(18.71)	(59.20)	(5.47)		
$[Sm(HBBP\text{-}ED)_2(H_2O)_2]_n$	Reddish	776	3.54	19.34	58.73	5.44	1.72	>300
$[C_{38}H_{42}O_8Sm]_n$	Brown		(73)	(19.36)	(58.73)	(5.43)		
$[Gd(HBBP\text{-}ED)_2(H_2O)_2]_n$	Reddish	783	3.74	20.08	58.21	5.40	7.90	>300
$[C_{38}H_{42}O_8Gd]_n$	Brown		(75)	(20.10)	(58.20)	(5.38)		
$[Tb(HBBP\text{-}ED)_2(H_2O)_2]_n$	Reddish	784	3.34	20.22	58.09	5.38	9.50	>350
$[C_{38}H_{42}O_8Tb]_n$	Brown		(72)	(20.20)	(58.10)	(5.36)		
$[Dy(HBBP\text{-}ED)_2(H_2O)_2]_n$	Reddish	787	3.35	20.58	57.83	5.36	10.52	>350
$[C_{38}H_{42}O_8Dy]_n$	Brown		(67)	(20.60)	(57.80)	(5.33)		

HBBP-ED = poly[(2-hydroxy-4-butoxy benzophenone)ethylene].

this particular band comes from the absorbed water. The band due to –O–H stretching is less broad in the IR spectra of the polymer, suggesting the absence of absorbed water. The strong band of –C=O around 1635–1655 cm^{-1} and weak band of –O–H at 2740–2765 cm^{-1} indicate an intramolecular hydrogen bond. The band in the range of $1230 \pm 10\,cm^{-1}$ is attributed to –O–H in plane bending. The bands observed around the 1480–1510 cm^{-1}, 2940 cm^{-1} and 1020–1170 cm^{-1} regions are attributed to –C=C– stretching (aromatic) vibrations, $–CH_2–CH_2–$ group and –C–H in plane bending, respectively. In the spectra of each resin, a band observed around $890 \pm 10\,cm^{-1}$ is due to isolated hydrogen on the phenolic repeating unit of the polymer chain. The band around 750 cm^{-1} may be attributed to the mono-substituted benzene ring having five adjacent H atoms. The medium intensity band at 900–860 cm^{-1} shows the 1,2,3,4, 5-penta-substituted phenyl ring. The strong band observed around $1265 \pm 15\,cm^{-1}$ is attributed to the $Ph–O–C_4H_9$ ether linkage. The bands around $895 \pm 10\,cm^{-1}$ suggest that the linkage in the resin chain occurs through 3 and 5 positions of the monomer. The important IR frequencies of the polymeric ligand and its polychelates are shown in table 2 (figure 1). The –C=O stretching frequency in the resin is observed around 1655–1635 cm^{-1}, at lower frequency by 20–40 cm^{-1} in all the polychelates, suggesting –C=O → M coordination [15]. In the polychelates the bands observed around 465–480 and 540–550 cm^{-1} indicate the M–O bond, suggesting that phenolic and carbonyl groups are involved in bond formation with the metal. The proposed structure of the polymeric ligand is shown in scheme 2.

3.2. *^{1}H NMR spectra*

The ^{1}H NMR spectra of 2-hydroxy-4-butoxy benzophenone (HBBP), poly[(2-hydroxy-4-butoxy benzophenone)ethylene] H(HBBP-ED) and polychelates (M-HBBP-ED) are presented in table 3.

HBBP signals at $\delta = 12.48$, 3.7–3.9 and 6.7–8.5 ppm are due to –OH group *ortho* to (Ar–C=O), $–OCH_3$ *para* to (Ar–C=O) and aromatic ring protons, respectively [16].

H(HBBP-ED) signals at $\delta = 12.3$, 3.7–3.9 and 6.9–8.6 ppm are due to –OH group o*rtho* to (Ar–C=O), $–OC_4H_9$ *para* to (Ar–C=O) and aromatic ring protons, respectively. One broad signal at $\delta = 1.1–2.9$ ppm appears due to the presence of (Ar–C=O–Ar–$\underline{CH_2–CH_2}$–) protons. In all the polychelates the signal of the –OH group completely disappears, suggesting that bond formation takes place through the –OH o*rtho* to (Ar–C=O). Also, aromatic protons were shifted upfield by 0.1–0.3 ppm in the NMR spectra of the polychelates due to deshielding of the metal ion on the ligand proton.

3.3. *Vapor pressure osmometry*

The number average molecular weight ($\overline{M}n$) of the polymeric ligand(resin) samples were estimated by vapor pressure osmometry [17]. Dilute solutions of polymer samples were prepared to determine $\overline{M}n$. Four concentrations, 2.21, 4.42, 6.63 and 8.84 $g\,kg^{-1}$, were prepared in DMF. The VPO experiment was carried out for each concentration and the corresponding bridge output reading in millivolts was noted as 26.00, 49.00, 70.00 and 91.00, respectively. The plot of millivolts *versus* concentration was drawn.

Table 2. Infrared spectra of the polymeric ligand and its polychelates (cm^{-1}).[a]

Compound	ν(O–H)	ν(–CH_2) bridge	ν(C=O) chelate	ν(C=C) romatic	ν(Ar–O–R) ether linkage	Penta-substituted Ph ring	ν(M–OH)
$(HBBP\text{-}ED)_n$	3300–3550 b	2871 w	1635 s	1510–1490 m	1265–1273 m	884 m	–
$[La(HBBP\text{-}ED)_2(H_2O)_2]_n$	3300–3550 b	2930 w	1608 s	1498 m	1258 m	861 s	480 m
$[Pr(HBBP\text{-}ED)_2(H_2O)_2]_n$	3300–3550 b	2930 w	1608 s	1508 m	1258 m	878 s	475 m
$[Nd(HBBP\text{-}ED)_2(H_2O)_2]_n$	3300–3550 b	2932 w	1610 s	1502 m	1257 m	890 s	473 m
$[Sm(HBBP\text{-}ED)_2(H_2O)_2]_n$	3300–3550 b	2928 w	1606 s	1500 m	1256 m	867 s	481 m
$[Gd(HBBP\text{-}ED)_2(H_2O)_2]_n$	3300–3550 b	2927 w	1608 s	1504 m	1258 m	873 s	486 m
$[Tb(HBBP\text{-}ED)_2(H_2O)_2]_n$	3300–3550 b	2930 w	1606 s	1501 m	1256 m	862 s	468 m
$[Dy(HBBP\text{-}ED)_2(H_2O)_2]_n$	3300–3550 b	2934 w	1610 s	1510 m	1265 m	868 s	479 m

[a] b = broad, m = medium, s = strong, w = weak.

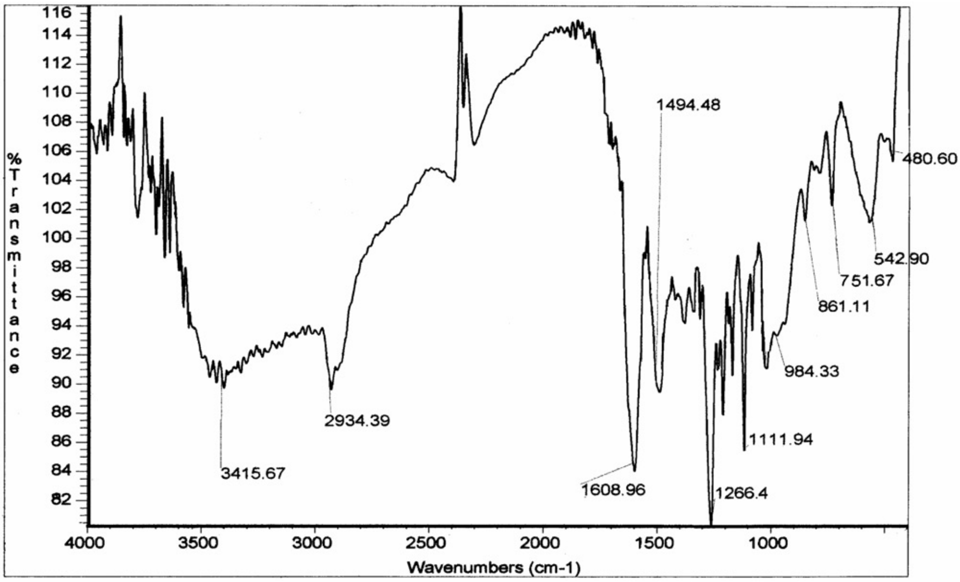

Figure 1. IR spectra of [(2-hydroxy-4-butoxy benzophenone)ethylene] resin.

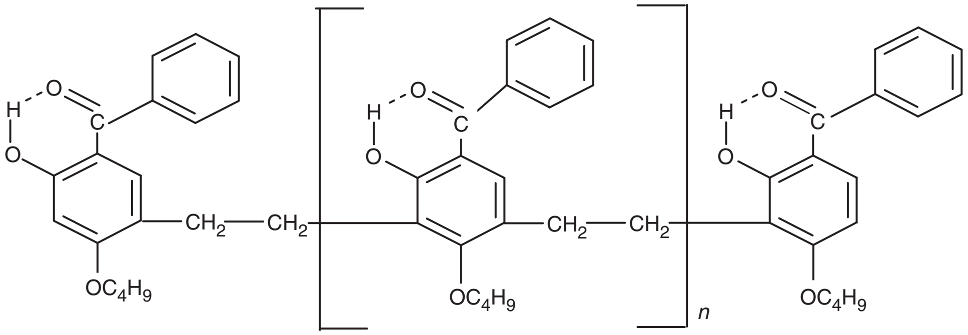

Scheme 2. Proposed structure of the polymeric ligand.

With the help of the slope (11.12) and the VPO constant K (1.15×10^4), the $\overline{M}n = 1349\,g\,mol^{-1}$ of the polymer was calculated.

3.4. *Thermogravimetric analyses*

Thermogravimetric analyses (TGA) of the resin and polychelates revealed that the rate of decomposition of the polychelate is higher than that of the parent resin, indicating strong intramolecular hydrogen bonding in the polymer. The absence of such hydrogen bonding in the polychelate favors reduction in thermal stability of polychelates compared to the parent resin; metal ions accelerate decomposition of the polychelates. According to Nikolaev *et al.* [18] water eliminated above 150°C is due to coordination to the metal ion. The water in the complexes is coordinated, indicated by cumulative % weight loss and thermal data presented in table 4.

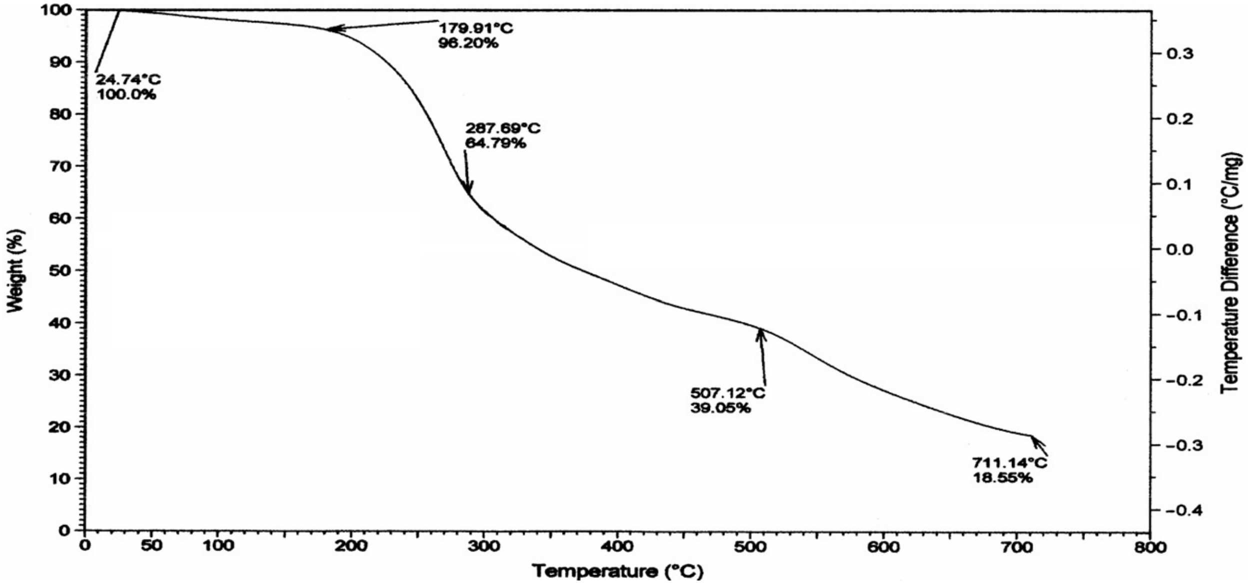

Figure 2. TGA of [Pr(2-hydroxy-4-butoxy benzophenone)ethylene] polychelate.

Table 3. ^{1}H NMR data of the polymeric ligand and its polychelates (δ, ppm).

	(δ ppm)			
Ligand/polychelates	–OH	Aromatic protons	$-CH_2-CH_2-$	$-OC_4H_9$
HBBP	11.5–12.5	6.7–8.5	–	3.7–3.9
$(HBBP\text{-}ED)_n$	11.7–12.3	6.9–8.6	1.1–2.9 (broad)	3.7–3.9
$[La(HBBP\text{-}ED)_2(H_2O)_2]_n$	–	6.84–8.58	1.1–2.9 (broad)	3.6–3.9
$[Pr(HBBP\text{-}ED)_2(H_2O)_2]_n$	–	6.81–8.55	1.1–2.9 (broad)	3.6–3.9
$[Nd(HBBP\text{-}ED)_2(H_2O)_2]_n$	–	6.77–8.6	1.1–2.9 (broad)	3.6–3.9
$[Sm(HBBP\text{-}ED)_2(H_2O)_2]_n$	–	6.79–8.56	1.1–2.9 (broad)	3.6–3.9
$[Gd(HBBP\text{-}ED)_2(H_2O)_2]_n$	–	6.81–8.5	1.1–2.9 (broad)	3.6–3.9
$[Tb(HBBP\text{-}ED)_2(H_2O)_2]_n$	–	6.86–8.62	1.1–2.9 (broad)	3.6–3.9
$[Dy(HBBP\text{-}ED)_2(H_2O)_2]_n$	–	6.78–8.57	1.1–2.9 (broad)	3.6–3.9

Table 4. Cumulative weight loss data of the polymeric ligand and its polychelates at various temperature (°C).

Compound	100	150	200	250	300	350	400	450	500	550	600
$(HBBP\text{-}ED)_n$	0.40	0.52	0.70	2.70	7.50	12.10	15.95	24.50	35.05	50.20	60.96
$[La(HBBP\text{-}ED)_2(H_2O)_2]_n$	1.85	2.44	10.60	12.80	15.75	20.35	26.74	32.52	38.33	43.60	46.23
$[Pr(HBBP\text{-}ED)_2(H_2O)_2]_n$	1.60	2.14	5.53	17.45	38.63	47.21	52.68	57.09	60.33	66.57	72.80
$[Nd(HBBP\text{-}ED)_2(H_2O)_2]_n$	1.37	2.41	10.05	19.31	30.26	36.75	44.99	51.78	58.37	64.83	68.02
$[Sm(HBBP\text{-}ED)_2(H_2O)_2]_n$	1.54	2.81	9.55	15.07	19.12	25.06	33.63	41.20	48.27	55.20	60.13
$[Gd(HBBP\text{-}ED)_2(H_2O)_2]_n$	1.01	2.12	9.87	31.76	56.27	61.59	67.43	72.53	78.15	83.27	83.48
$[Tb(HBBP\text{-}ED)_2(H_2O)_2]_n$	1.87	2.93	10.54	19.46	42.91	50.14	56.49	61.16	65.15	72.27	78.07
$[Dy(HBBP\text{-}ED)_2(H_2O)_2]_n$	1.39	2.01	10.41	18.78	19.79	20.54	24.51	32.84	39.00	46.74	54.01

3.5. *Differential scanning calorimetry (DSC)*

Differential scanning calorimetry (DSC) analysis of the polymeric resin is used to study mechanism and kinetics of curing, a valuable tool for investigating kinetic and thermal parameters like activation energy (E) for curing, heat of reaction (ΔH), pre-exponential factor ($\log z$), order of reaction (n) and curing characteristics such as degree of curing, temperature and duration of curing for phenolic resins [19].

From a single DSC scan of HBBP-PD, we obtained the temperature at which the reaction was activated $(T_i) = 140.64^\circ C$, maximum $(T_p) = 190.56^\circ C$, completed $(T_f) = 215^\circ C$ and curing temperature $T_f - T_i = 74.36^\circ C$ along with kinetic parameters by using the Borchardt Daniels method [20]. The major advantage of the Borchardt Daniels method is the determination of activation energy $(E_a) = 120.23\,\text{kJ mol}^{-1}$, pre-exponential factor $(\log z) = 33.29\,\text{min}^{-1}$, heat of reaction $(\Delta H) = 13.40\,\text{J gm}^{-1}$ and order of reaction $(n) = 5.64$ from only a single DSC scan.

3.6. *Electronic spectra and magnetic measurements*

The electronic spectra of all the polychelates exhibited two additional bands in the region 260–300 nm and 445–465 nm. The first band occurs in the spectra of the polymeric ligand, assigned to $\pi \rightarrow \pi_1^*$ and $\pi \rightarrow \pi_2^*$ [21]. The second band is assigned to the polymeric ligand → Ln(III) transitions in all the polychelates. The La(III) polychelate was diamagnetic as expected. The electronic spectra of Pr(III), f^3,

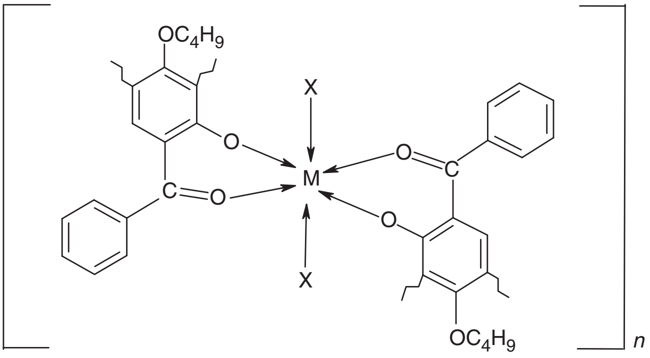

M = La(III), Pr(III), Nd(III), Sm(III), Gd(III), Tb(III) and Dy(III); X = H_2O

Scheme 3. Proposed structure of the polymeric chelate.

polychelate exhibits absorption at 21,324, 20,865, 19,458 and 17,715 $\mathrm{cm^{-1}}$, assigned to $^3H_4 \rightarrow {}^3P_2$, $^3H_4 \rightarrow {}^3P_1$, $^3H_4 \rightarrow {}^3P_0$ and $^3H_4 \rightarrow {}^1D_2$ transitions of Pr(III) in an octahedral environment, due to large crystal field with magnetic moment 3.70 BM. The Nd(III) polychelate is paramagnetic as expected for f^4 system. Bands were obtained at 18,970, 17,645, 14,273 and 9,885 $\mathrm{cm^{-1}}$ for $^4I_{9/2} \rightarrow {}^2G_{9/2}$, $^4I_{9/2} \rightarrow {}^4G_{5/2}$, $^4I_{9/2} \rightarrow {}^2S_{3/2}$, $^4I_{9/2} \rightarrow {}^2S_{3/2}$, and $^4I_{9/2} \rightarrow {}^4F_{5/2}$ transitions of Nd(III) in octahedral geometry. Bands at 23,168, 22,920 and 23,880 $\mathrm{cm^{-1}}$ for polychelate are assigned to $^4H_{5/2} \rightarrow {}^4F_{9/2}$, $^4H_{5/2} \rightarrow {}^6p_5$ and $^4H_{5/2} \rightarrow {}^4I_{11/2}$ transitions of Sm(III) in octahedral geometry due to large crystal field splitting, and the polychelate is paramagnetic. The magnetic moment 1.71 BM is expected. The Gd(III) and Tb(III) polychelates were paramagnetic 7.89 and 9.52 BM as expected for six coordinated polychelates. The electronic spectra of Dy(III) f^{10} polychelates exhibits absorption at 27,750 $\mathrm{cm^{-1}}$ assigned to $^6H_{15/2} \rightarrow {}^6H_{13/2}$ transition of Dy(III) in octahedral geometry due to large crystal field splitting. From above study the proposed structure of polychelate is as shown in scheme 3.

4. Ion exchange

The purified resin sample HBBP-ED was powdered to pass a 300 mesh screen and used in all experiments for ion-exchange study.

The batch equilibration method was used. The details of the procedure for selectivity of lanthanide(III) metal ions by the resin is similar to an earlier report [22].

The selectivity of HBBP-ED toward lanthanide(III) metal ions has been studied under the influence of electrolyte on uptake of metal ion, effect of pH on metal binding capacity, rate of metal uptake and distribution ratio (K_D) of metal ions over the range of pH. The results are shown in tables 5–8.

4.1. *Influence of an electrolyte on uptake of metal ion*

The influence of Cl^-, NO_3^-, ClO_4^- and SO_4^{2-} ions at various concentrations on the metal-resin equilibrium has been studied (table 5). The amount of metal ion taken up by

Table 5. Effect of electrolyte concentration on metal ion adsorption capaticity of HBBP-ED resin.

Metal ions	Electrolyte (Mol. lit^{-1})	Metal ion uptake (meq g^{-1}) in presence of electrolyte			
		$NaNO_3$	NaCl	Na_2SO_4	$NaClO_4$
La^{3+}	0.05	0.49	0.43	0.48	0.50
	0.10	0.57	0.50	0.40	0.59
	0.50	0.68	0.63	0.33	0.71
	1.00	0.85	0.72	0.27	0.79
Pr^{3+}	0.05	0.52	0.46	0.45	0.41
	0.10	0.61	0.63	0.37	0.59
	0.50	0.75	0.72	0.24	0.64
	1.00	0.89	0.84	0.20	0.75
Nd^{3+}	0.05	0.50	0.44	0.43	0.52
	0.10	0.54	0.61	0.32	0.63
	0.50	0.67	0.69	0.26	0.68
	1.00	0.90	0.83	0.16	0.76
Sm^{3+}	0.05	0.57	0.45	0.54	0.55
	0.10	0.68	0.61	0.45	0.67
	0.50	0.76	0.72	0.37	0.70
	1.00	0.86	0.82	0.25	0.78
Gd^{3+}	0.05	0.51	0.44	0.60	0.52
	0.10	0.62	0.59	0.47	0.64
	0.50	0.75	0.68	0.40	0.78
	1.00	0.89	0.80	0.33	0.82
Tb^{3+}	0.05	0.58	0.41	0.62	0.52
	0.10	0.66	0.65	0.55	0.64
	0.50	0.74	0.72	0.44	0.78
	1.00	0.86	0.83	0.36	0.82
Dy^{3+}	0.05	0.50	0.48	0.54	0.48
	0.10	0.66	0.66	0.40	0.59
	0.50	0.70	0.74	0.36	0.66
	1.00	0.89	0.81	0.29	0.80

Resin, HBBP-ED = 50 mg; $Mt(NO_3)_2$ = 2 mL, 0.1 M; volume of electrolyte solution = 40 mL; time = 24 h; temperature = 30°C; pH of the medium = 5.6.

Table 6. Effect of pH on metal ion binding capacity with HBBP-ED resin.

Metal ion	Metal ion uptake (meq g^{-1})				
	pH of the medium				
	3.0	3.5	4.0	5.0	5.5
La^{3+}	0.41	0.52	0.57	0.70	0.78
Pr^{3+}	0.43	0.50	0.58	0.74	0.81
Nd^{3+}	0.38	0.53	0.61	0.72	0.83
Sm^{3+}	0.43	0.53	0.62	0.75	0.85
Gd^{3+}	0.43	0.55	0.61	0.71	0.77
Tb^{3+}	0.40	0.52	0.60	0.72	0.79
Dy^{3+}	0.42	0.54	0.60	0.72	0.80

Resin, HBBP-ED = 50 mg; $Mt(NO_3)_2$ = 2 mL, 0.1 M; volume of electrolyte solution = 40 mL; time = 24 h; temperature = 30°C.

the resin increases with an increase in concentration of NO_3^-,CIO_4^-, and Cl^- and decreases with an increase in concentration of SO_4^{2-}. Sulphate forms rather strong chelates with metal, while nitrate and chloride are weaker. Therefore, the influence of NO_3^-, ClO_4^- and Cl^- is less on the metal chelate equilibrium than SO_4^{2-}.

Table 7. Rate of metal ion uptake by HBBP-ED as a function of time*.

	Metal ion uptake (meq g^{-1})						
	pH of medium (3–5.5)						
Time in hours	La^{3+}	Pr^{3+}	Nd^{3+}	Sm^{3+}	Gd^{3+}	Tb^{3+}	Dy^{3+}
1	40.26	20.32	33.56	41.18	31.54	38.72	34.65
2	49.70	32.60	41.12	47.26	38.64	44.32	40.12
3	55.42	42.75	56.47	52.20	45.83	50.76	49.79
4	62.75	51.91	65.21	65.41	51.77	60.28	56.87
5	70.90	62.98	74.25	73.22	59.99	74.91	63.33
6	85.20	72.36	80.14	88.34	66.71	85.82	72.80
7	90.15	81.72	86.54	90.62	72.68	90.43	82.41

Resin, HBBP-ED = 50 mg; $Mt(NO_3)_2$ = 2 mL, 0.1 M; volume of electrolyte solution = 40 mL; time = 24 h; temperature = 30°C, *assuming 100% equilibrium is established after 24 h.

Table 8. Distribution ratio of ions adsorbed by HBBP-ED and remaining in solution at equilibrium.

	Distribution ratio (K_D)				
	pH of the medium				
Metal ion	3.0	3.5	4.0	5.0	5.5
La^{3+}	62.00	120.88	240.42	320.12	412.66
Pr^{3+}	72.55	140.32	264.47	351.56	443.21
Nd^{3+}	48.16	125.72	242.70	331.56	410.11
Sn^{3+}	71.97	174.22	273.87	361.85	442.51
Gd^{3+}	46.78	134.72	257.98	343.31	428.35
Tb^{3+}	57.66	145.47	226.85	324.93	404.27
Dy^{3+}	80.32	172.94	284.54	390.43	476.17

Resin, HBBP-ED = 50 mg; $Mt(NO_3)_2$ = 2 mL, 0.1 M; volume of electrolyte solution = 40 mL; time = 24 h; temperature = 30°C.

4.2. *Effect of pH on metal binding capacity*

The results of selected metal uptake are presented in table 6. The rate of metal ion uptake depends on the nature of metal ion. The study was restricted to maximum pH = 6, due to hydrolysis of metal ions at higher pH. The relative amount of metal adsorbed by the resin increases with increasing pH of the medium.

4.3. *Evaluation of the rate of metal uptake*

To determine the time required to reach equilibrium under given experimental conditions, a series of experiments were carried out, in which the metal uptake by the chelating resin was estimated. It is assumed that at 25°C and under given conditions, the state of equilibrium is established in 24 h. The rate of metal uptake is expressed as percentage of equilibrium (table 7). If "X" mg of metal ions were adsorbed, after 1 h and "Y" mg of metal ions were adsorbed at equilibrium, i.e. after 24 h, $X \times 100/Y$ would be the measure of percentage of equilibrium attained after one hour. It can be seen that the rate increases for the first 3–4 h for La(III), Nd(III) and Sm(III) and equilibrium is attained after 24 h for all metal ions.

4.4. *Evaluation of distribution ratio (K_D) of metal ions over the wide range of pH*

The distribution of each of the metal ions [La^{3+}, Pr^{3+}, Nd^{3+}, Sm^{3+}, Gd^{3+}, Tb^{3+} and Dy^{3+}] between the resin phase (solid) and aqueous phase (liquid) is estimated at appropriate pH, using 1.0 M $NaNO_3$ solution. The experiments were carried out from 3 to 5.5 pH. The amount of the metal ion which remained in the aqueous phase was estimated. The original metal ion concentration is known, and the metal ion adsorbed by the resin was estimated. The results are shown in table 8. The distribution ratio 'K_D' has been calculated from the following equation.

$$K_D = \frac{\text{Amount of metal adsorbed on resin}}{\text{Amount of metal in solution}} \times \frac{\text{Volume of solution}}{\text{Weight of resin}}$$

The effect of pH on the amount of metal distributed between two phases can be explained by the results shown in table 6, increasing for La^{3+}, Pr^{3+}, Nd^{3+}, Sm^{3+}, Gd^{3+}, Tb^{3+} and Dy^{3+} as the pH increases. The value of distribution ratio for given pH depends on the nature of the polymeric ligand (resin).

5. Antimicrobial activity

The bacterial strains of *Escherichia coli*, *Bacillus subtilis*, *Staphylococcus aureus* and yeast strains *Saccharomyces cerevisiae* were tested with the polymeric ligand and their polychelates. The effect of the compound in the growth media were investigated by standard microbiological parameters. The concentration of the compounds was kept at 500 ppm during the experiment. The bacterial culture was maintained on N-agar (N-broth, 2.5% w/v agar). The yeast culture was maintained on MGYP in 3% (w/v) agar, malt extract 0.3% (w/v), glucose 1.0% (w/v), yeast extract 0.3% (w/v) and peptone 0.5% (w/v) in distilled water and the pH was adjusted to 6.7–7.3. All were subcultured every fourth night and stored at 0–5°C.

5.1. *Media composition*

For the growth and test of bacteria and yeast, the N-broth and MGYP media were used as shown below.

N-broth	Peptone 0.6% (6.0 gm), NaCl 0.15% (1.5 gm) and beef extract 0.15% (1.5 gm) were dissolved in 1 L distilled water and pH was adjusted to 6.7–7.3.
MGYP	Malt extract (3.0 gm), glucose (10.0 gm), yeast extract (3.0 gm) and peptone (5.0 gm) were dissolved in 1 L distilled water and pH was adjusted to 5.5.

5.2. *Inoculum preparation*

For bacterial and yeast cultures, a loop of cell mass from pregrown slants was inoculated into sterile N-broth tubes containing 15 mL medium and incubated on a shaker at 150 rpm and 37°C for 24 h to obtain sufficient cell density (i.e. 1×10^8 cells mL^{-1}).

5.3. *Screening of compounds for their antimicrobial activity*

Antimicrobial activity was checked by the agar diffusion method [23]. Sterile, melted N-agar was poured into a sterile empty petri plate and allowed to solidify. A ditch was prepared with the help of a sterile scalpel on opposite ends, with one for control (solvent without compound) and the other for the test sample. The pregrown cultures were streaked parallel from one ditch to another. One of the ditches was filled with respective components dissolved in DMSO at concentrations ranging from 50–1000 ppm. Then after, the plates were transferred to the refrigerator for 10 min to allow the sample to diffuse out from the ditch and into the agar before organisms start growing followed by incubation at 37°C for 24 h. The next day the distance in millimeters (mm) from the ditch was measured as a parameter of inhibition.

The polymeric ligand and metal complexes were studied for their antimicrobial activity against standard bacterial strains of *E. coli*, *B. subtilis*, *S. aureus* (bacteria) and *S. cerevisiae* (yeast) at different concentrations ranging from 50–1000 ppm to find the minimum concentration of the ligand and the polychelates, which inhibits the microbial growth; minimum concentration of 500 ppm was found. The inhibition of growth from the ditch was measured in millimeters (mm) and the results are shown in table 9. The polymeric ligand was biologically active and the polychelates showed significantly enhanced antibacterial activity against one or more bacterial species in comparison to the uncomplexed polymeric ligand. Chelation tends to make the ligands more potent bactericidal agents than the parent ligand. In the chelate, the positive charge of the metal is partially shared with the donor atoms of the ligand with π-electron delocalization over the whole chelate ring [24]. This, in turn, increases the lipophilic character of the metal and favors its permeation through the lipoid layers of

Table 9. Antimicrobial activity data of the polymeric ligand and its polychelates.

	Microbial species			
	Bacteria			Yeast
Ligand/polychelates	*E. coli*	*B. subtilis*	*S. aureus*	*S. cerevisiae*
$(\mathrm{HBBP\text{-}ED})_n$	+	−	−	+
$[\mathrm{La(HBBP\text{-}ED)_2(H_2O)_2}]_n$	+++	++	++	+++
$[\mathrm{Pr(HBBP\text{-}ED)_2(H_2O)_2}]_n$	+++	+	+	+++
$[\mathrm{Nd(HBBP\text{-}ED)_2(H_2O)_2}]_n$	++	++	++	++
$[\mathrm{Sm(HBBP\text{-}ED)_2(H_2O)_2}]_n$	+++	++	++	+++
$[\mathrm{Gd(HBBP\text{-}ED)_2(H_2O)_2}]_n$	+++	++	++	+++
$[\mathrm{Tb(HBBP\text{-}ED)_2(H_2O)_2}]_n$	+++	++	++	+++
$[\mathrm{Dy(HBBP\text{-}ED)_2(H_2O)_2}]_n$	++	++	++	+++
Control (DMSO)	−	−	−	−

Inhibition diameter in mm (% inhibition): +, 6−10 (27−45%); ++ 10−14 (45−64%); +++, 14−18 (64−82%); ++++, 18−22 (82−100%). Percent inhibition values are relative to inhibition (22 mm) with 100% inhibition; −, no inhibition.

the bacterial membrane. Besides this, other factors may also influence the antimicrobial activity.

6. Conclusion

On the basis of elemental analyses, IR, thermogravimetric analyses, ^{1}H NMR spectra, magnetic properties and vapor pressure osmometry, the proposed geometry of the complex is as shown in scheme 3. The resin has good binding capacity for the lanthanide ions at different conditions employed for the ion-exchange study and good antimicrobial activity compared to free polymeric ligand. The thermal stability of polychelates is less than the polymeric ligand. The results revealed that the resin can be used as an ion-exchanger and antimicrobial agent.

Acknowledgement

The authors thank the Head of the Department of Chemistry and Bioscience, Sardar Patel University, Vallabh Vidyanagar, for providing laboratory facilities.

References

[1] E.L. Cooper, M.K. Hass, J.F. Mattie. *Appl. Radiat. Isot.*, **46**, 1159 (1995).
[2] N. Dumont, A. Favre-Réguillon, B. Dunjic, M. Lemaire. *Sep. Sci. Technol.*, **31**, 1001 (1996).
[3] J.D. Joshi, N.B. Patel, S.D. Patel. *J. Macro. Molecular Sci. Part A, PAC*, **43**, 1179 (2006).
[4] S.I. Al-Gharabli, K.A.K. Ebraheem, M.S. Mubarak. *Saudi Chem. Soc.*, **5**, 399 (2001).
[5] K.A.K. Ebraheem, M.S. Mubarak, S.I. Al-Gharabli. *J. Macromol. Sci.-Pure Appl. Chem. A*, **39**, 217 (2002).
[6] A.I. Ismail, K.A.K. Ebraheem, M.S. Mubarak, F.I. Khalili. *Solvent Extr. Ion Exch.*, **21**, 125 (2003).
[7] M. Draye, K.R. Czerwinski. *Separat. Sci. Technol.*, **35**, 1117 (2000).
[8] L.K. Orazzhanova, M.G. Yashkarova, L.A. Bimendina, S.E. Kudaibergenov. *J. Appl. Polym. Sci.*, **87**, 759 (2003).
[9] T. Mizuta, M. Onishi, K. Miyoshi. *Organometallics*, **19**, 5005 (2000).
[10] B.L. Rivas, H.A. Maturana, M.J. Molina, M.R. Gomej-Anton, M. Rosa, I.F. Pierola. *J. Appl. Polym. Sci.*, **67**, 1109 (1998).
[11] H. Tusa, A. Paavola, R. Harjula, J. Letho. 8th International Conference of Radioactive Waste Management and Environmental Remediation, Vol 3, p. 42, (2001).
[12] K.R. Won, W.J. Change, H. Kim, Y.M. Koo, J.H. Hahn. *Electrophoresis*, **24**, 3253 (2003).
[13] S. Varvara, L. Muresan, I.C. Popescu, G. Maurin. *Hydrometallurgy*, **75**, 147 (2004).
[14] P. Soroushian, M. Elzafraney, H. Chowdhury, G. Sarwar, F. Aouadi. *Polymer Composites*, **26**, 679 (2005).
[15] S. Nursen, K. Ebru, S. Bekir, O. Aulin. *J. Macro. Molecular Sci. Part A, PAC*, **43**, 1227 (2006).
[16] R.M. Silverstein, F.X. Webster. *Spectrometric Identification of Organic Compounds*, 6th Edn, John Wiley & Sons, Inc., New York (1998).
[17] A. Eliassi, H. Modarress. *Euro. Poly. J.*, **37**, 1487 (2001).
[18] A.V. Nikolaev, V.A. Logvinenko, L.T. Myachina. *Thermal Analysis*, p. 779, Academic Press, New York (1969).
[19] R.M. Greshnm. *Tribology and Lubrication Tech.*, **59**, 28 (2003); CA 139(26), 397638u, 2003.
[20] H.J. Borchardt, F. Daniels. *J. Amer. Chem. Soc.*, **41**, 79 (1957).
[21] A. Kriza, A. Reiss, S. Florea, T. Carproin. *J. Ind. Chem. Soc.*, **77**, 207 (2000).
[22] J.D. Joshi, N.B. Patel, S.D. Patel. *Iranian Polymer J.*, **15**, 219 (2006).
[23] R.Y. Stanier. *Introduction to the Microbial World*, 5th Edn, pp. 16–20, Prentice Hall, Inc., NJ (1986).
[24] Z.H. Chohan, S. Kausar. *Metal-Based Drugs*, **7**, 17 (2000).